Preparation of Low-Density Macrocellular Tin Dioxide Foam with Variable Window Size

Qincui Gu, Keiji Nagai,* Takayoshi Norimatsu, Shinsuke Fujioka, Hiroaki Nishimura, Katsunobu Nishihara, Noriaki Miyanaga, and Yasukazu Izawa

Institute of Laser Engineering, Osaka University, 2-6 Yamada-oka, Suita, Osaka 565-0871, Japan

Received October 5, 2004

Low-density porous tin dioxide (∼0.5 g/cm^3) was prepared from a $SnCl_4$/ethanol/H_2O mixture and polystyrene (PS) template. Such a low density made the as-synthesized tin dioxide act as a promising target material for laser-induced extreme ultraviolet (EUV) emission. The resulting structure of the as-synthesized tin dioxide (SnO_2) was a cellular foam, which was composed of large cells (ca. 10^3 nm, large macropores) interconnected by windows (ca. 10^2 nm, small macropores). Scanning electron microscope images showed that SnO_2 particles of ∼10 nm constituted the cell wall. The space among particles formed mesopores, which were about 7 nm estimated by nitrogen adsorption−desorption isotherm measurements. Therefore, the as-prepared SnO_2 showed a hierarchical porous system from macropores to mesopores. The window size on a submicrometer scale was tunable in the range of ∼480−200 nm by changing the molar ratio of ethanol to $SnCl_4$ in tin source solution from 2:1 to 10:1. By consideration that the windows originated from the tight contact area among the PS spheres, some parameters affecting the contacting area among the PS spheres were investigated in order to analyze the effect of ethanol content on the widow size. The wettability of the tin source solution on the PS particle film and the viscosity of the tin source solution were found to be the main reasons responsible for the variable window size. Another observed phenomenon was the change in the SnO_2 filling area from the complete filling of voids to a mere coating of the colloidal spheres as the ethanol content was increased, that is, a template transition from a volume template to a surface template was realized by changing the ethanol content. The mechanism was discussed in detail.

Introduction

Porous material with a hierarchical pore system is an emerging technology due to applications as catalysts, separation and mass transportation.[1−4] Many efforts have been made to prepare silica-based materials with a bimodal or trimodal pore system.[5−9] The development of hierarchical nonsiliceous porous materials is also essential for exploring new application fields.[10] Among the various porous metal oxides, tin dioxide is one of the most useful materials, which can be applied in many technological fields including solar cells,[11] gas sensors,[12,13] lithium battery,[14] separation,[15] etc. Recently, it has been proved that low-density tin oxide (SnO_2) (1.5 g/cm^3) is an important target material for producing narrow extreme ultraviolet (EUV) emission with a high conversion efficiency.[16,17] EUV lithography (EUVL) will be a key technology for carving electric circuit nodes less than several tens of namometers into silicon wafers in succeeding years.[18] To prepare SnO_2 with density lower than 1.5 g/cm^3 is very important for EUV emission target material fabrication. A wide range of techniques has been exploited to synthesize tin dioxide, such as sol−gel, spray pyrolysis, chemical vapor deposition (CVD), magnetron sputtering, evaporation of metallic tin in an oxygen atmosphere, sonication, anodic oxidation process, supramolecular template technique, etc.[11,12,19−23] Most of these techniques provide tin

* To whom correspondence should be addressed. Phone: +81-(6)-6879-8778. Fax: +81-(6)-6877-4799. E-mail: knagai@ile.osaka-u.ac.jp.

(1) Holland, B. T.; Abrams, L.; Stei, A. *J. Am. Chem. Soc*. **1999**, *121*, 4308.
(2) Davis, S. A.; Burkett, S. L.; Mendelson, N. H.; Mann, S. *Nature* **1997**, *385*, 420.
(3) Yang, P.; Deng, T.; Zhao, D.; Feng, P.; Pine, D. *Science* **1998**, *282*, 2244.
(4) Velev, O. D.; Tessier, P. M.; Lenhoff, A. M.; Kaler, E. W. *Nature* **1999**, *401*, 548.
(5) Huerta, L.; Guillem, C.; LaTorre, J.; Beltrán, A.; Beltrán, D.; Amorós, P. *Chem. Commun.* **2003**, 1448.
(6) Suzuki, K.; Ikari, K.; Imai, H. *J. Mater. Chem.* **2003**, *13*, 1812.
(7) Bagshaw, S. A. *Chem. Commun*. **1999**, 1785.
(8) Haskouri, J. E.; Zárate, D.; Guillem, C.; Amorós, P.; Caldés, M.; Marcos, M. D.; Beltrán, D.; LaTorre, J.; Amorós, P. *Chem. Mater*. **2002**, *14*, 4502.
(9) Zhang, B. J.; Davis, S. A.; Mann, S. *Chem. Mater.* **2002**, *14*, 1369.
(10) Miyat, H.; Itoh, M.; Watanabe, M.; Noma, T. *Chem Mater.* **2003**, *15*, 1334.
(11) Srivastava, D. N.; Chappel, S.; Palchik, O.; Zaban, A.; Gedanken, A. *Langmuir* **2002**, *18*, 4160.
(12) Chen, F. L.; Liu, M. L. *Chem. Commun.* **1999**, 1829.
(13) Manorama, S. V.; Gopal Reddy, C. V.; Rao, V. J. *Nanostructured Mater*. **1999**, *11*, 643.
(14) Lytle, J. C.; Yan, H.; Ergang, N. S.; Smyrl, W. H.; Stein, A. *J. Mater. Chem.* **2004**, 1616.
(15) Schmidt-Winkel, P. S.; Lukens, W. W.; Zhao, D. Y.; Yang, P. D.; Chmelka, B. F.; Stucky, G. D. *J. Am. Chem. Soc.*, **1999**, *121*, 254.
(16) Nagai, K.; Nishimura, H.; Okuno, T.; Hibino, T.; Matsui, R.; Tao, Y. Z.; et al. *Trans. Mater. Res. Soc. Jpn*, **2004**, *29*(3), 943.
(17) Chou, I. W.; Daido, H.; Yamagami, S.; Nagai, K.; Norimatsu, T.; Takabe, H. *J. Opt. Soc. Am. B*, **2000**, *17*, 1616.
(18) Nishimura, H.; Shigemori, K.; Nakai, M. *J. Plasma Fusion Res.* **2004**, *80*, 325.
(19) Shin, H. C.; Dong, J.; Liu, M. L. *Adv. Mater.* **2004**, *16*, 237.
(20) Ulagappan, N.; Rao, D. N. R. *Chem. Commun.* **1996**, 1685.
(21) Qi, L.; Ma, J.; Cheng, M.; Zhao, Z. *Langmuir* **1998**, *14*, 2579.

10.1021/cm048259u CCC: $30.25
Published on Web 02/08/2005

dioxide with a microporous or mesoporous structure. In addition, the colloidal-crystal templating method is an effective approach for preparing macroporous metal oxide materials.[14,24,25] In the present study, the polystyrene (PS) sphere template technique is introduced in order to prepare low-density tin dioxide with hierarchical pore systems from mesopores to macropores.

The resulting structure of the porous metal oxides using the colloidal-crystal template method is called cellular foam (CF), which is composed of large spherical cells interconnected by opening windows to create a continuous pore system.[15,26] Such a structure easily affords low-density porous metal compounds. In addition, many applications of porous materials are strongly dependent on the windows, and therefore, it is important to control the pore structure and the window size. Up to now, only a few examples about controlling the window size have been reported.[25,27−29] Schmidt et al. obtained siliceous mesostructured cellular foams with variable window size by adding ammonium fluoride to the oil-in-water microemulsion.[27] Lukens et al. also prepared mesocellular silica foams with tunable windows by varying the silica-to-surfactant ratio, where the obtained window size was controlled in the range of mesopore from several to 20 nm.[28] The effects of alkoxide dilution with ethanol were investigated for macroporous silica, titania, and zirconia samples by Holland et al.[29] Their result showed that the window size was enlarged by the increasing dilution. By use of a poly(methyl methacrylate) (PMMA) sphere template, Lytle et al. obtained a porous tin dioxide with different window sizes and SnO_2 crystalline grain sizes by calcination at different temperatures.[14] In the present study, the hierarchical porous SnO_2 with a variable window size was synthesized by diluting the tin precursor solution with ethanol, while the size of the grains constituting the SnO_2 crystal remained almost unaffected. The dilution effect is discussed in detail.

Experimental Part

Materials. Styrene and potassium persulfate ($K_2S_2O_8$) were commercially supplied by Aldrich and the Nacarai Chemical Co. (Kyoto), respectively. Anhydrous tin tetrachloride ($SnCl_4$) with a 99.99% purity was purchased from Katayama Chemical Industrial Co. The ethanol (99.5%, Kishida Chemical Co.) was used without further purification. The water was purified by a Yamato WG 262 distilling system and used for the synthesis of the PS and hydrolysis of the tin precursor.

Synthesis. 1. Synthesis of Surfactant-Free PS. PS particles were synthesized by a surfactant-free emulsion polymerization process (90 wt % dispersed aqueous phase) with $K_2S_2O_8$ as the initiator (the weight ratio of $H_2O/K_2S_2O_8 = 1200:1$).[29] The reaction was carried out at 80 °C in a N_2 atmosphere for 24 h, and the stirring speed was maintained at 250 rpm. The resulting PS spheres were filtered through a mesh to remove any large agglomerates. The PS sphere diameter was determined to be 1.3 μm by scanning electron microscopy (SEM). The PS spheres remained suspended in the mother liquor until needed.

The prepared PS sphere emulsion (4 mL) was dropped onto a glass substrate (20 cm^2) to obtain a sphere template film. Before they were dropped, the glass substrates were treated with 98% sulfuric acid overnight and then rinsed with deionized water.

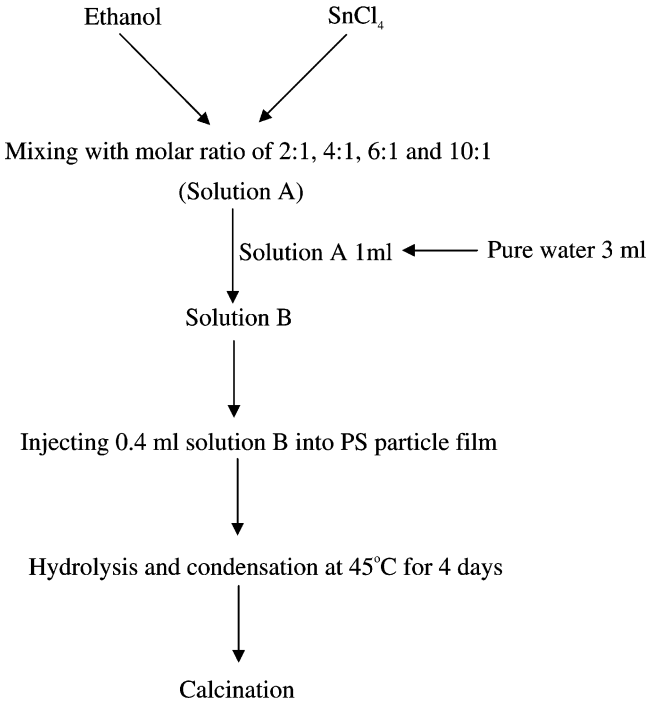

Figure 1. Preparation of porous SnO_2.

2. Preparation of porous SnO_2. The procedure of preparing the porous SnO_2 is shown in Figure 1. $SnCl_4$ was used as the starting tin source and added to ethanol at the molar ratios of ethanol/$SnCl_4$ of 2:1, 4:1, 6:1, and 10:1. The resulting solution was denoted as solution A. The possible chemical reaction is presented by eq 1, in which a partial ligand exchange takes place. Pure water was mixed with solution A in a volume ratio of 3:1 at room temperature, and this prepared solution was denoted as solution B. A partial hydrolysis reaction might take place after the water was added, as shown in eq 2. However, the condensation reaction of the partially hydrolyzed species was expected to be hindered by the existence of a large amount of ethanol.[28,30]

$$SnCl_4 + xC_2H_5OH \leftrightarrows SnCl_{4-x}(OC_2H_5)_x + xHCl \quad (1)$$

$$SnCl_{4-x}(OC_2H_5)_x + (y+z)H_2O \leftrightarrows SnCl_{4-x-y}(OC_2H_5)_{x-z}(OH)_{y+z} + yHCl + zC_2H_5OH \quad (2)$$

Subsequently, the as-prepared PS template was infiltrated by solution B (0.02 mL/cm^2) due to capillary forces and the following hydrolysis and condensation processes were carried out at 45 °C for 4 days. The composite was finally calcined at 400 °C for 5 h to decompose the PS, and porous SnO_2 was obtained. The above process is illustrated in Figure 2.

(22) Severin, K. G.; Abdel-Fattah, T. M.; Pinnavaia, T. J. *Chem. Commun*, **1998**, 1471.
(23) Thierry, T.; Odile, B.; Bernard, J.; Gil, V. *Chem. Mater.* **2003**, *15*, 4691.
(24) Zhong, Z.; Yin, Y.; Gates, B.; Xia, Y. *Adv. Mater.* **2000**, *12*, 206.
(25) Shchukin, D. G.; Caruso, R. A. *Chem. Mater.* **2004**, *16*, 2287.
(26) Gu, Z. Z.; Uetsuka, H.; Takahashi, K.; Nakajima, R.; Onishi, H.; Fujishima, A.; Sato, O. *Angew. Chem., Int. Ed.* **2003**, *42*, 894.
(27) Schmidt-Winkel, P.; Lukens, W. W.; Yang, P. D.; Margolese, D. I.; Lettow, J. S.; Ying, J. Y.; Stucky, G. D. *Chem. Mater.* **2000**, *12*, 686.
(28) Lukens, W. W.; Yang, P. D.; Stucky, G. D. *Chem. Mater.* **2001**, *13*, 28.
(29) Holland, B. T.; Blanford, C. F.; Do, T.; Stein, A. *Chem. Mater*. **1999**, *11*, 795.
(30) Mauro, E.; Marco, A.; Luciana, M.; Gabriella, L.; Pietro, S.; Lorenzo, V. *J. Am. Ceram. Soc.* **2001**, *84*, 48.

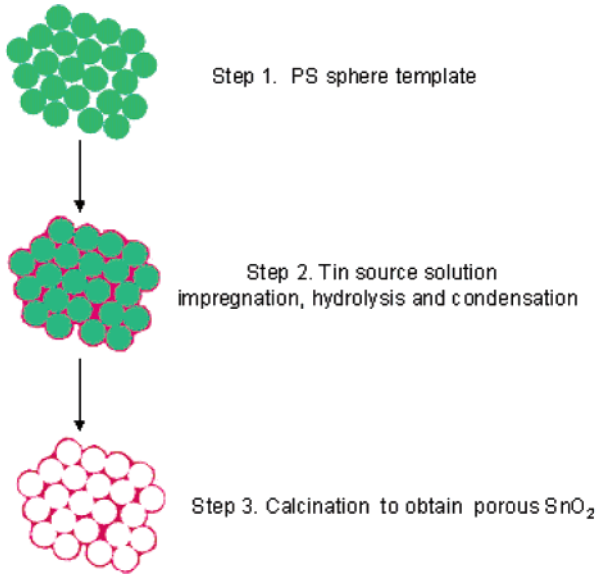

Figure 2. Schematic diagram of preparation procedure of porous SnO_2 using PS as a template.

Characterization. SEM images were obtained using a JEOL JSM-7400F field-emission scanning electron microscope operated at an accelerating voltage of 2 kV in the gentle-beam mode (ultralow accelerating voltage and high resolution). The PS sample was coated with platinum to improve the conductivity when observed by the SEM.

Wide-angle X-ray diffraction (WAXD) measurements were carried out on a Rigaku RINT2500HF+ WAXD spectrometer with Cu Kα radiation at 1.54 Å. The average grain size of the tin dioxide was calculated on the basis of the Scherrer equation as shown in eq 3

$$L = \frac{k\lambda}{\beta \cos \theta} \tag{3}$$

where k is the Scherrer shape factor that equals 0.94, λ is the X-ray wavelength of 1.54 Å, β is the peak full width at half-maximum in radians, and θ is the diffraction peak position. Jade 6 XRD processing software was used to analyze the crystalline phase and grain size. The grain size was calculated by fitting the ⟨211⟩ diffraction peak of SnO_2.

The nitrogen adsorption−desorption isotherms were measured at 77 K using a high-speed gas sorption analyzer (Quantachrome Nova 1000). Before the analysis, each sample was degassed at 373 K for 6 h under vacuum. The adsorption data at the relative pressure of $P/P_0 = 0.30$ was used to calculate the single point Brunauer−Emmett−Teller (BET) surface area. The pore size distribution was obtained from the desorption branch of the isotherms using the Barrett−Joyner−Halenda (BJH) method.

The viscosity of the tin source solution (1 mL) was measured using a DV-E digital viscometer (Tokyo Keiki).

The contact-angle measurements were performed in order to determine the wettability of the tin source solution on the PS film. A drop of the tin source solution with a 1-mm diameter was dropped onto the PS film. The angle measurement was carried out after the solution droplet was in contact with PS film for 20 s, and the measurements were repeated three times for each sample.

Results and Discussion

1. Characterization of Porous SnO_2. Figure 3 shows the SEM images of the PS sphere template and corresponding porous SnO_2 after decomposing the PS. As seen in Figure 3a, the PS spheres are closely stacked together and the average sphere diameter is 1.3 μm. The porous SnO_2 with a CF structure is obtained after calcination, as presented in Figure 3b. The magnified CF structure in the inset of Figure 3b clearly shows that the as-synthesized SnO_2 is composed of large spherical cells (~10^3 nm) interconnected by small windows (~hundreds nanometers).[15] The circle and the arrow in the inset of Figure 3b point out the position of the cell and the window, respectively. Because the cell size (~10^3 nm) is in the range of macropores,[31] the terms of macrocellular foams (abbreviated as MACFs) is adopted to describe the resulting structure of the porous SnO_2. The cells in the MACFs correspond to the area occupied by the template spheres, and the windows mainly originate from the tightly contacting regions among the PS spheres where the source solution cannot infiltrate.[28] The window formation mechanism is illustrated in Figure 4. In Figure 4a, the PS spheres are coated by the tin compound during the infiltration process, while the tight contact area among the PS spheres has no tin coating because the tin source solution cannot penetrate into it. After calcination, the void space left in the original contact area constitutes the window.

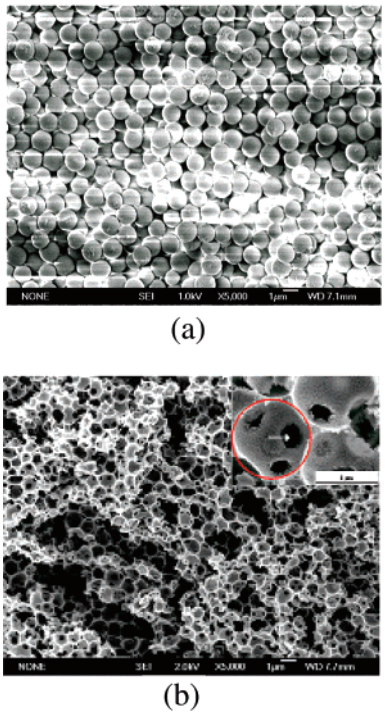

Figure 3. SEM images of (a) PS microspheres and (b) porous SnO_2 after calcination. (Inset: the magnified MACFs structure. The molar ratio of ethanol/$SnCl_4$ solution is 4:1.)

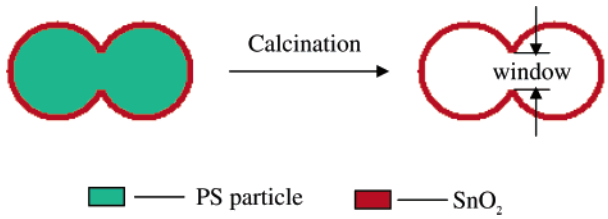

Figure 4. Schematic diagram of window formation mechanism.

The magnified SEM image in Figure 5 indicates that the cell wall is composed of about 10-nm particles. The

(31) Gates, B.; Yin, Y. D.; Xia, Y. N. *Chem. Mater.* **1999**, *11*, 2827.

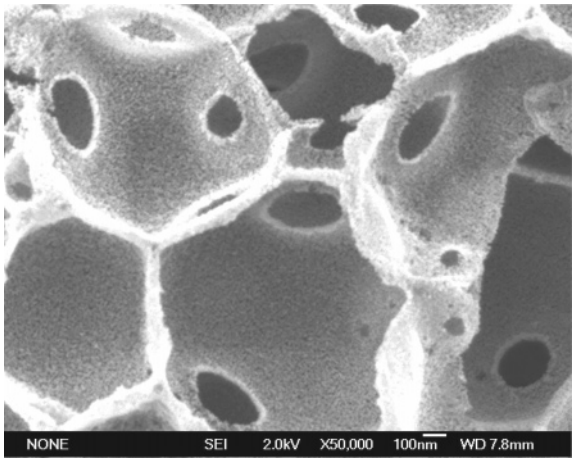

Figure 5. The magnified SEM image of porous SnO_2 with crystalline particles in the cell wall (using the sample prepared with 6:1 ethanol/tin tetrachloride solution).

interparticle void space differentiated by the SEM is smaller than 10 nm, which consists of the mesopore structure of porous SnO_2. Therefore, it can be concluded that the as-prepared porous SnO_2 shows a hierarchical pore system at three different scale length, that is, mesopore−the interparticle space (<10 nm), small macropore−window (~10^2 nm), and large macropore−cell (~10^3 nm).

The nitrogen adsorption−desorption isotherm was measured in order to characterize the mesopore structure in the cell wall. Figure 6a presents the isotherm curve of the porous SnO_2 prepared from the tin solution with a 6:1 (molar ratio) of ethanol to $SnCl_4$. Other samples prepared from different tin solutions showed a similar isotherm property. Such an isotherm was assigned to Type IV according to the IUPAC classification.[32] A hysteresis of Type H1 at higher relative pressures can be found in the isotherm curve, which is typical for mesoporous materials that exhibit capillary condensation and evaporation. This kind of hysteresis also indicates that the porous material has a large pore size with a narrow size distribution.[33] The result of the BJH analysis shown in Figure 6b indicates that the calcined SnO_2 exhibits a mesopore structure with an average pore size of 7 nm, which is in agreement with the SEM observation (<10 nm). The single-point BET surface area was calculated to be 53 m^2/g at the relative pressure of $P/P_0 = 0.30$.

WAXD measurements were carried out to investigate the crystallinity of the same SnO_2 sample as used in the nitrogen isotherm experiments. These results are presented in Figure 7. The diffraction peaks situated at $2\theta = 26$, 33, 37, and 51° are assigned to the diffraction of ⟨110⟩, ⟨101⟩, ⟨200⟩, and ⟨211⟩ of the cassiterite, respectively. The grain size is estimated to be 2.4 nm from the broadening of the ⟨211⟩ diffraction peak using Scherrer equation (eq 3). Therefore, the as-prepared porous SnO_2 is composed of nanocrystalline SnO_2 grains after calcination. The ~10 nm particles observed by SEM are actually the aggregation of the small crystalline grains (~2.4 nm).

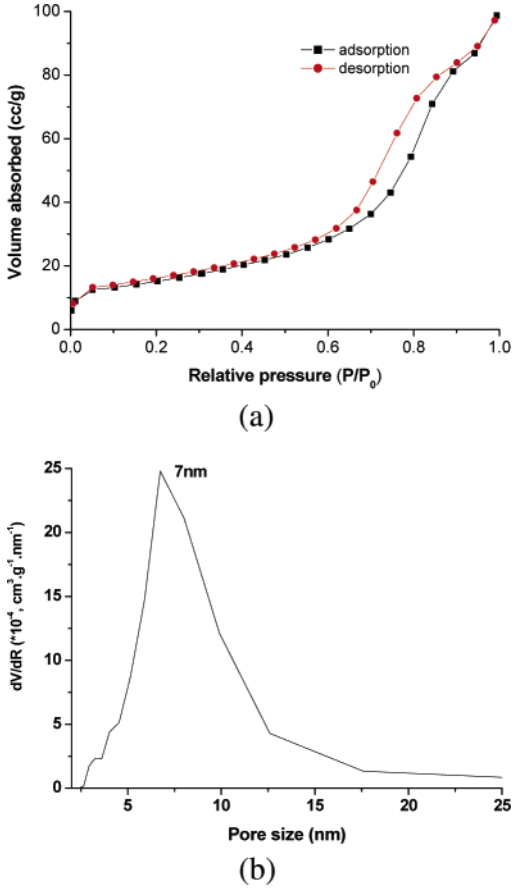

Figure 6. (a) Nitrogen adsorption−desorption isotherm; (b) pore-size distribution plot (using the sample prepared with 6:1 ethanol/tin tetrachloride solution).

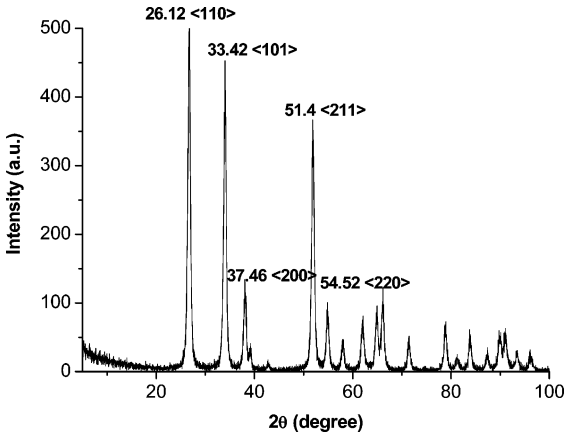

Figure 7. WAXD pattern of as-synthesized porous SnO_2 with 6:1 ethanol/tin tetrachloride solution.

In summary, the combined techniques of the PS template method and sol−gel chemistry make the as-prepared SnO_2 have a macrocellular foam structure with a hierarchical pore system and a nanocrystalline cell wall.

2. Effect of Ethanol Content. As listed in Table 1, the tin source solutions with different molar ratios of ethanol to $SnCl_4$ were infiltrated into the PS particle films. The morphology of the as-synthesized SnO_2 was found to significantly depend on the molar ratio of ethanol to $SnCl_4$, as presented in Figure 8. It can be easily seen from parts a−d of Figure 8 that the window size is an important parameter controlled by the ethanol content. As the molar

(32) Sing, K. S. W.; Everett, D. H.; Haul, R. A. W.; Moscou, L.; Pierotti, R. A.; Rouquérol, J.; Siemieniewska, T. *Pure Appl. Chem.* **1985**, *57*, 603.
(33) Greg, S. J.; Sing, K. S. W. In *Adsorption, Surface Area and Porosity*; Academic Press: New York, 1982.

Table 1. Effect of Molar Ratio of Ethanol to $SnCl_4$ on the Window Size and Average Density

run	molar ratio of ethanol to $SnCl_4$	density of solution B (g/ cm^3)	viscosity of solution B ($\times 10^{-6}$ m^2/s)	window size[a] (nm)	average density[b] of tin oxide (g/cm^3)
1	2	1.274	8.7	480	0.51 (7.3%)[c]
2	4	1.219	7.2	360	0.47 (6.8%)
3	6	1.147	6.7	230	0.52 (7.5%)
4	10	1.104	6.4	200	0.49 (7.1%)

[a] Determined from SEM observation. The data were calculated from the average of 20 windows and the error bar is ±15 nm. [b] Determined by measuring the mass and volume of as-prepared porous SnO_2. [c] Calculated from the density of bulk SnO_2 (6.95 g/cm^3)

ratio of ethanol to $SnCl_4$ was increased from 2:1 to 10:1, the window size is variable in the range of ~480−200 nm.

The window is a typical and important structure parameter for cellular foam materials. By consideration that the windows originated from the tight contact area among the PS spheres (illuminated in Figure 4), some parameters affecting the contact area among the PS spheres were investigated to analyze the effect of the ethanol content on window size. First, viscosity experiments were performed to confirm the improved infiltrating capability of the tin source solution into the PS spheres as the ethanol content increased. The viscosity data are shown in Table 1. It can be seen that the viscosity of the tin source solution decreased from 8.7×10^{-6} m^2/s to 6.4×10^{-6} m^2/s when the molar ratio of ethanol to $SnCl_4$ increased from 2:1 to 10:1. The decreased viscosity makes tin source solution easily and quickly infiltrate into the voids among PS spheres due to capillary force. As a result, the contact area of the PS spheres decreased and much more PS surface was coated by the tin source solution. By consideration of the formation mechanism of the windows (see Figure 4), a smaller window should be obtained in porous SnO_2 prepared from a higher ethanol content source solution. Second, the wettability of the tin source solution on the PS particle film was investigated by contact-angle measurement. This result is shown in Figure 9. It can be seen from parts a−d of Figure 9 that the contacting angle decreased from 77 to 50° when the molar ratio of ethanol to $SnCl_4$ changed from 2:1 (run 1) to 10:1 (run 4), which means that the wettability of the tin source solution with PS spheres was experimentally confirmed to be improved by the higher ethanol content. The improved wettability facilitates the tin source solution to easily cover and penetrate into the PS particles. As a result, a higher surface area of PS spheres was covered by the tin source solution and the penetrated depth of the PS sphere should be increased. Therefore, the smaller window should be observed for a higher ethanol content in the tin source solution.

To further elucidate the effect of the ethanol content on the window size, tin oxide was prepared from the tin source solution of $SnCl_4/H_2O$ (1:3 volume ratio) without ethanol. The SEM image of the as-prepared SnO_2 shown in Figure 10 illustrates that only an ~1 μm pore is formed in this sample, which indicates that only the vacancies among the PS spheres are filled with the tin source solution and the PS particle surface remains uncovered. The morphology of the as-prepared porous SnO_2 from the $SnCl_4/H_2O$ solution is not a CF structure. The poor wettability of the tin solution due to the lack of ethanol is considered to be the main reason for this kind of morphology. Therefore, the improvement in the wettability by ethanol is important for the cellular foam structure and the window size.

Except for the window size, the interspace among the SnO_2 CFs is another parameter affected by the ethanol content, as confirmed by the SEM images in Figure 8. It can be seen from Figure 8a that the interspace among the SnO_2 CFs is small and occupied by the SnO_2 nanocrystals, while it is large and void in the interspace among the SnO_2 cell foams in parts c and d of Figure 8, as it was indicated that there existed different template effects depending on the ethanol content. Zakihidov et al. classified the template effect into the volume template and the surface template.[34] The volume template results from the complete filling of the pores with source solution and the surface template from the mere coating of the colloidal spheres. Therefore, the volume template acts as the main template method for the lower ethanol content in the tin source solution, and tin compounds should cover both the particle surface and the voids, as seen in the SEM image of parts a and b of Figure 8. When the ethanol content was increased in the tin source solution, the improved wettability of the tin source solution on the PS particles will induce the tin source solution to cover and easily penetrate into the particle surface. In this case, the surface template controls the templating process, as seen in the SEM images of the PS/SnO_2 composite before calcination (Figure 11). The samples used in Figure 11a and b are the PS/SnO_2 composites prepared from the tin source solution with 2:1 and 10:1 ethanol/$SnCl_4$ ratios, respectively. It can be seen from Figure 11a that both the PS surface and the voids among the PS spheres are covered by SnO_2, which indicates that the volume template controls the templating process. In contrast, only the PS surface is coated by SnO_2 for the higher ethanol content solution (see Figure 11b), that is, the surface template effect is induced by the higher ethanol content. In addition, the slow gelation process caused by the higher ethanol content also contributes to the conversion of the template effect to the surface template. The reason for this would be as follows: the evaporation of ethanol would occur before the gel network was completely formed. The ethanol contained in the interspace among the PS particles evaporates faster than the ethanol covering the surface of PS. For the higher ethanol content in the tin solution, much of the ethanol evaporated before completion of the gel network because the gelation process was prolonged. As a result, the surface template effect was observed before the calcination and the open cell morphology of SnO_2 was formed after the calcination.

It can be concluded from the above discussion that the ethanol content affects both the window size and the filling of the interspace, while there are still other parameters not influenced by the dilution of tin tetrachloride. In our experiment the particle size and the density of the as-prepared SnO_2 were found to be independent of the ethanol content. Figure 12 presents the magnified SEM images of the as-

(34) Zakhidov, A. A.; Baughman, R. H.; Iqbal, Zr.; Cui, C. X.; Marti, J.; Ralchenko, V. G. *Science* **1998**, *282*, 897.

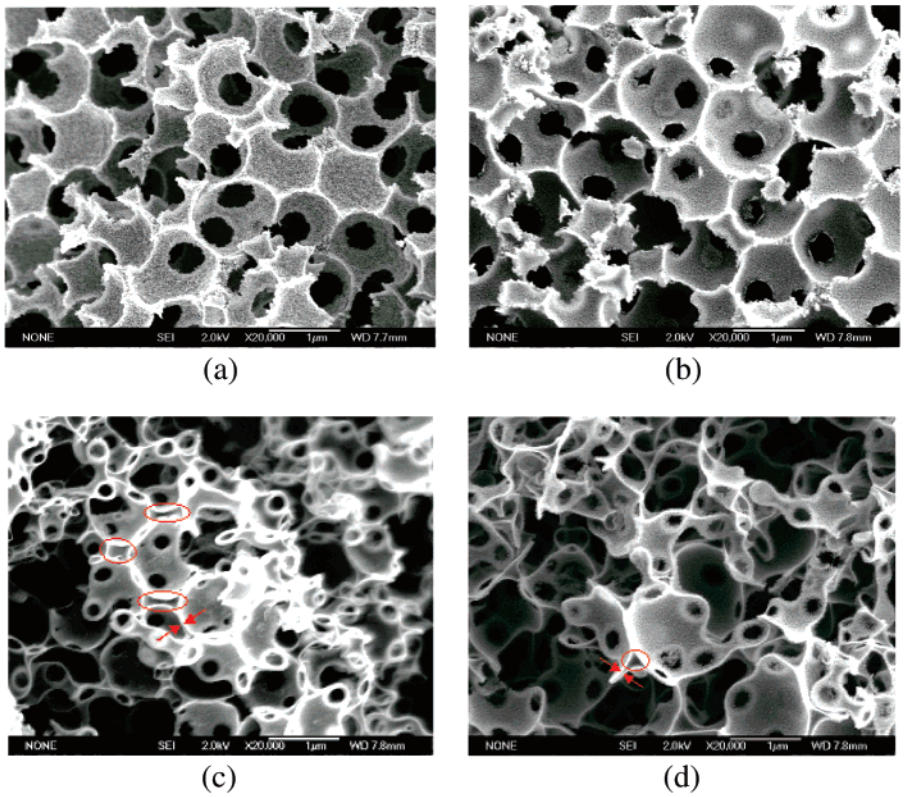

Figure 8. SEM images of porous SnO_2 prepared with different tin source solution (a) run 1; (b) run 2; (c) run 3; (d) run 4.

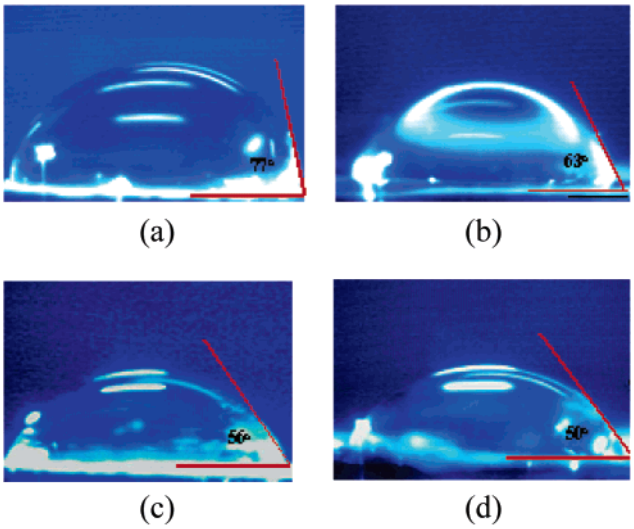

Figure 9. Photographs of contact angle of different tin source solution with PS film. (a) Run 1; (b) run 2; (c) run 3; (d) run 4.

prepared SnO_2 from different tin source solution concentrations. It can be seen that the cell wall is composed of SnO_2 particles. The particle size is constant at about 10 nm, which is almost unaffected by the different tin source solution concentrations. In the work of Lytle et al., a tunable window size of porous SnO_2 was also obtained by calcinating samples at different temperatures.[14] At the same time, the particle size and the crystallinity were also distinctly changed as a result of the different calcination temperatures. On the contrary, our present work provides another choice for preparing porous SnO_2 with a variable window size, but the particle size and crystallinity remain constant.

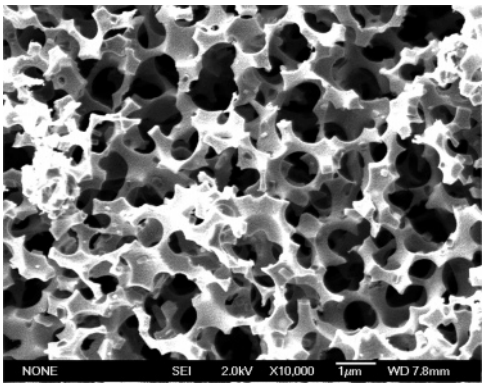

Figure 10. SEM image of as-prepared SnO_2 from $SnCl_4/H_2O$ source solution (volume ratio of $SnCl_4/H_2O$ = 1:3).

Density is one of the important parameters for porous materials, especially for laser plasma target applications.[15,35,36] Some of the present authors showed that a low-density SnO_2 (1.5 g/cm^3) prepared from $SnCl_4$ and the PS template induces a narrower EUV emission peak while maintaining a similar conversion efficiency.[16] Recent experiments revealed that such a low-density target provides a small laser plasma without readsorption due to the surrounding plasma.[37] The density of the present porous SnO_2 is about 0.50 g/cm^3 (see Table 1), which is 7% of the bulk SnO_2 density (6.95 g/cm^3). Such a low-density SnO_2 is a promising target material to get a much narrower EUVL emission profile. In

(35) Nagai, K.; Cho, B. R.; Hashishin, Y.; Norimatsu, T.; Yamanaka, T. *Jpn. J. Appl. Phys., Part B* **2002**, *41*, L431.
(36) Nagai, K.; Norimatsu, T.; Izawa, Y. *Fusion Sci. Technol.* **2004**, *45*, 79.
(37) Tao, Y.; Sohbatzadeh, F.; Nishimura, H. *Appl. Phys. Lett*, **2004**, *85*, 191.

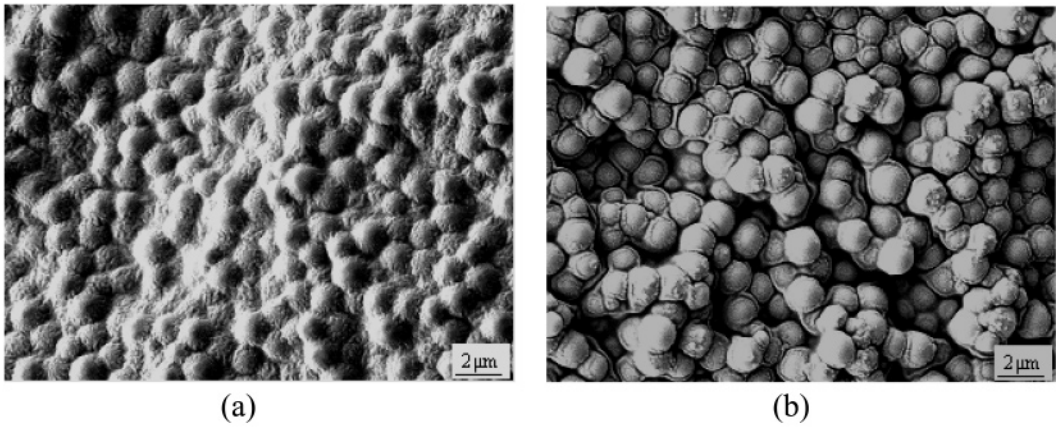

Figure 11. SEM images of PS/SnO_2 composite prepared from tin source solution with ethanol/$SnCl_4$ molar ratio of (a) 2:1 and (b) 10:1.

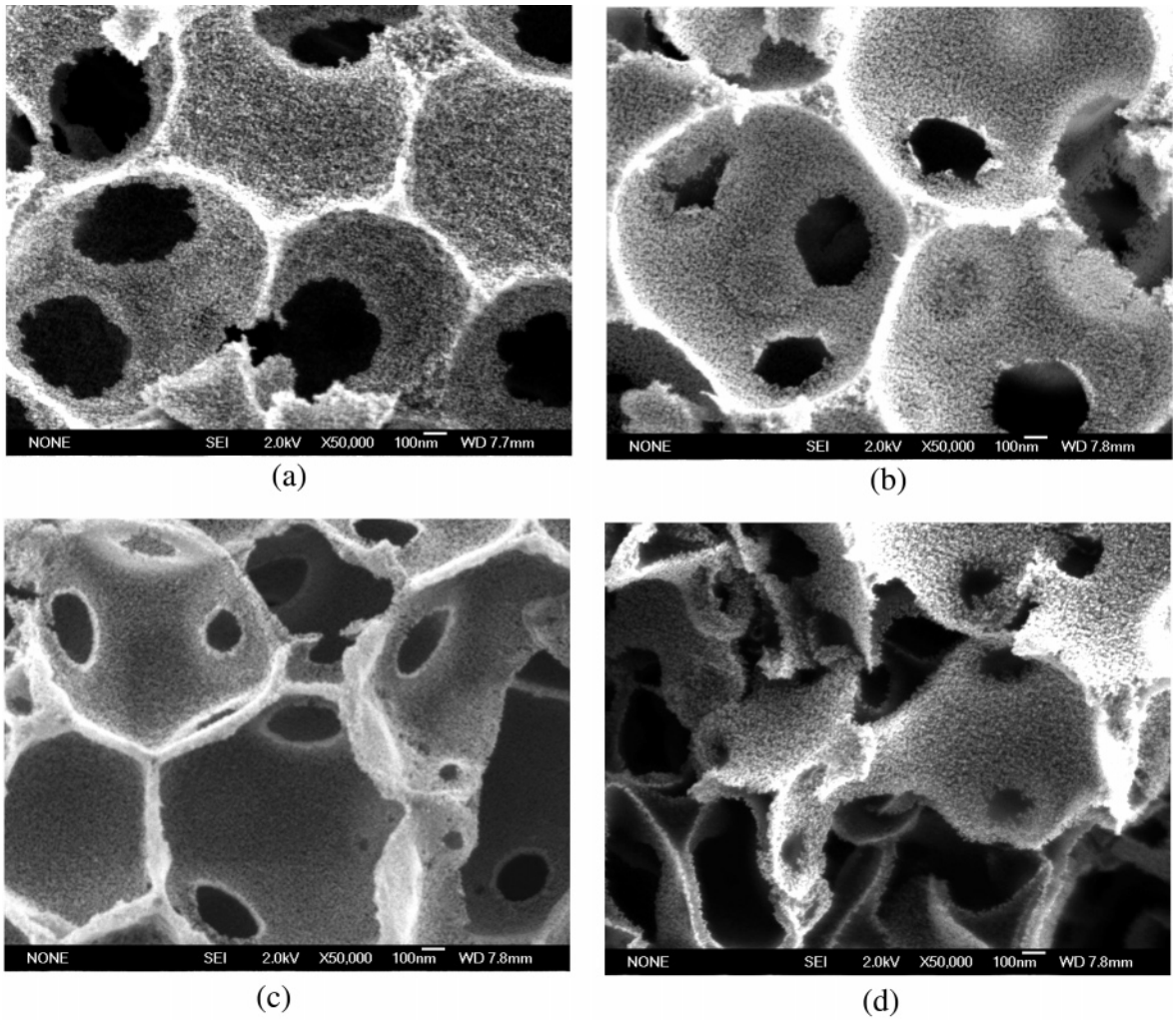

Figure 12. The magnified SEM images of SnO_2 (a) run 1; (b) run 2; (c) run 3; (d) run 4.

addition, as listed in Table 1, the density of the as-prepared SnO_2 remains at ~0.5 g/cm^3 although the window size and their morphology are different from each other, as is useful for investigating the structure effect of SnO_2 on the EUV emission for the same density.

Conclusions

The combination technique of PS template and sol−gel chemistry was introduced to prepare an extremely low density tin dioxide (~0.5 g/cm^3) with $SnCl_4$/ethanol/H_2O as the tin precursor solution. The as-prepared SnO_2 showed a CF structure with a hierarchical pore system, that is, a mesopore−interparticle space, a small macropore−window, and a large macropore−cell. The cell wall was composed of 10-nm SnO_2 particles, which were aggregates of nanocrystalline grains of about 2.4 nm. As an important parameter of the CF structure, the window size was variable in the range of ~480−200 nm as the molar ratio of ethanol to $SnCl_4$ in the tin precursor solution was changed from 2:1 to 10:1. The improved wettability of the tin solution on the PS particle

film and low viscosity of the tin source solution would be the reasons for the decreasing window size as more ethanol was added to the starting solution. Another effect related to the ethanol content was the change in template effect from the volume template to the surface template as the ethanol content was increased and correspondingly, the morphology of the as-prepared SnO_2 cell foam was also changed. Except the parameters affected by the ethanol content, some other parameters such as the crystalline particles constituting the SnO_2 cell wall and the density of the as-prepared SnO_2 remained independent of the ethanol content in the tin source solution.

Acknowledgment. A part of this work was performed under the auspices of the Ministry of Education, Culture, Science and Technology, Japan under the contract subject "Leading Project for EUV lithography source development".

CM048259U